Identification of Amino Acid Substitutions that Confer a High Affinity for Sulfaphenazole Binding and a High Catalytic Efficiency for Warfarin Metabolism To P450 2C19†

Frank Jung,‡ Keith J. Griffin, Wu Song,§ Toby H. Richardson,|| Mierha Yang, and Eric F. Johnson*

Department of Molecular and Experimental Medicine, The Scripps Research Institute, La Jolla, California 92037

Received July 15, 1998; Revised Manuscript Received September 21, 1998

ABSTRACT: Human cytochrome P450s 2C9 and 2C19 metabolize many important drugs including tolbutamide, phenytoin, and (*S*)-warfarin. Although they differ at only 43 of 490 amino acids, sulfaphenazole (SFZ) is a potent and selective inhibitor of P450 2C9 with an IC_{50} and a spectrally determined binding constant, K_S, of <1 μM. P450 2C19 is not affected by SFZ at concentrations up to 100 μM. A panel of CYP2C9/2C19 chimeric proteins was constructed in order to identify the sequence differences that underlie this difference in SFZ binding. Replacement of amino acids 227−338 in 2C19 with the corresponding region of 2C9 resulted in high-affinity SFZ binding ($K_S \sim 4$ μM) that was not seen when a shorter fragment of 2C9 was substituted (227−282). However, replacement of amino acids 283−338 resulted in extremely low holoenzyme expression levels in *Escherichia coli*, indicating protein instability. A single mutation, E241K, which homology modeling indicated would restore a favorable charge pair interaction between K241 in helix G and E288 in helix I, led to successful expression of this chimera that exhibited a $K_S < 10$ μM for SFZ. Systematic replacement of the remaining differing amino acids revealed that two amino acid substitutions in 2C19 (N286S, I289N) confer high-affinity SFZ binding ($K_S < 5$ μM). When combined with a third substitution, E241K, the resulting 2C19 triple mutant exhibited a high cataltyic efficiency for warfarin metabolism with the relaxed stereo- and regiospecificity of 2C19 and a lower K_M for (*S*)-warfarin metabolism (<10 μM) typical of 2C9.

Human P450s[1] 2C9 and 2C19 both metabolize a number of drugs that are of clinical importance such as tolbutamide (*2*), diazepam (*4*), phenytoin (*5*), and (*S*)-warfarin (*6*). Although they differ in only 43 of 490 amino acids, P450 2C9[2] displays more stringent steric requirements than P450 2C19. For example, only the (*S*)-enantiomer of warfarin is a substrate for P450 2C9 leading to hydroxylation of the 6 and 7 positions (*6, 7*), and phenytoin is stereospecifically oxidized in the pro- (*S*) ring (*5*). In contrast, P450 2C19 oxidizes both (*S*)- and (*R*)-warfarin at a larger number of sites (4′, 6, 7, and 8 positions) with a lower catalytic efficiency and hydroxylates both the pro-(*S*) and pro-(*R*) rings of phenytoin. 2C19 is also the major enzyme responsible for the 4′-hydroxylation of (*S*)-mephenytoin (*8, 9*) and is highly selective for the 5-hydroxylation of omeprazole (*10, 11*) while 2C9 exhibits very little activity toward either of these substrates. In addition, *in vitro* studies with human liver microsomes (*12*−*14*) and with heterologously expressed recombinant P450s (*15, 16*) have shown that P450 2C9 is selectively inhibited by submicromolar concentrations of sulfaphenazole (SFZ), whereas P450 2C19 is not inhibited by SFZ at concentrations up to 100 μM.

Roughly, 2%−5% of Caucasians and 15%−20% of Orientals do not express P450 2C19 as a result of the inheritance of two null alleles of the CYP2C19 gene (*3*). This can lead to greatly diminished metabolism of drugs such as (*S*)-mephenytoin that require efficient metabolism by P450 2C19 for normal clearance. In addition, allelic variation for the gene encoding P450 2C9 can result in diminished metabolism of other drugs such as the anti-coagulant (*S*)-warfarin (*17*) that places such patients at risk. Understanding the structural features of these two closely related enzymes that determine substrate specificity and efficient metabolism would allow the identification of the molecular characteristics of substrates that lead to relatively exclusive and efficient

† This work was supported by USPHS Grant GM31001 (E.F.J.) and a postdoctoral fellowship from the Deutsche Forschungsgemeinschaft (F.J.). Facilities for computer-assisted analysis, DNA sequencing, and the synthesis of oligonucleotides are supported in part by General Clinical Research Center Grant M01 RR00833 and by the Sam and Rose Stein Charitable Trust.

* To whom correspondence should be addressed: Eric F. Johnson, Ph.D., The Scripps Research Institute, Division of Biochemistry/NX 4, 10550 N. Torrey Pines Rd., La Jolla, CA 92037. Tel: 619 784-7918. Fax: 619 784-7981. E-mail: johnson@scripps.edu.

‡ Current affiliation: Fresenius Medical Care, Daimlerstr. 15, 61343 Bad Homburg, Germany.

§ Current affiliation: Applied BioTech, Inc., 10237 Flanders Ct., San Diego, CA 92121.

|| Current affiliation: Diversa Corporation, 10665 Sorrento Valley Road, San Diego, CA.

[1] Abbreviations: P450, cytochrome P450; IPTG, isopropyl-β-D-thiogalacto-pyranoside; CHAPS, 3-[(3-cholamidopropyl)-dimethyl-ammonio]-1-propanesulfonate; DLPC, L-α-dilauroyl-phosphatidylcholine; SFZ, sulfaphenazole.

[2] The amino acid sequences of the expressed P450 2C9 used in this study correspond to the previously published sequence designated "65" (*1*). The 2C19 sequence differed from the reported sequence (*1*) by a single amino acid substitution I330V (A → G substitution at nucleotide 991 of the cDNA). This substitution represents a second functional allele of P450 2C19 (*2, 3*).

10.1021/bi981704c CCC: $15.00 © 1998 American Chemical Society
Published on Web 10/28/1998

metabolism by one or the other enzyme and provide a foundation for the rational design of drugs whose clearance is less likely to be affected by genetic variation.

The objective of this study was to identify amino acid residues or key structural features of the protein that account for the selective high-affinity binding of SFZ to P450 2C9. Initially, a panel of 2C9/2C19 chimeras was generated to identify the smallest segment of P450 2C9 that would confer high-affinity SFZ binding. The hybrid proteins were expressed in *Escherichia coli*, partially purified, and subsequently analyzed for SFZ binding by optical difference spectroscopy. The catalytic competence of the chimeric proteins was assessed by measuring (*S*)- and (*R*)-warfarin metabolism in reconstitution assays. A minimal chimera (chimera G) that displayed high-affinity SFZ binding was identified, and systematic replacement of the remaining, differing residues by site-directed mutagenesis was then used to identify a minimal set of critical amino acid residues. Homology modeling of P450 2C9 and manual docking of SFZ in the model were used to guide the design and interpretation of site-directed mutagenesis experiments.

MATERIALS AND METHODS

Chemicals and Reagents. Restriction and DNA modification enzymes were obtained from New England Biolabs (Beverly, MA) or Stratagene (La Jolla, CA). Competent *E. coli* cells (Epicurian Coli XL1-Blue) and the QuickChange site-directed mutagenesis kit were purchased from Stratagene (La Jolla, CA). Other chemicals were obtained from Sigma (St. Louis, MO) unless otherwise indicated. SFZ was purchased from RBI (Natick, MA). (*S*)- and (*R*)-warfarin and the warfarin metabolites 4′-, 6-, 7-, and 8-hydroxywarfarin were purchased from Ultrafine Chemicals (Manchester, UK). (*S*)- and (*R*)-warfarin were converted into their sodium salts by adding an equimolar amount of 0.1 N NaOH and stored in aliquots of 5 mM stock solutions in 50 mM potassium phosphate buffer, pH 7.4, at −80 °C until use.

Construction of Chimeras and Site-Directed Mutagenesis. The design and characterization of plasmids for the expression of P450s 2C9 and 2C19 in *E. coli* have been described previously (*2*). Chimeric expression constructs were generated from the parent plasmids by exchange of restriction fragments using the following restriction endonuclease sites: *Sma*I (codon 227), *Eco*RI (codon 281), *Pst*I (codon 291), and *Sph*I (codon 338). The *Eco*RI site was introduced as a silent mutation into 2C9 by site-directed mutagenesis in order to match the respective site in 2C19. Site-directed mutagenesis was performed using the QuikChange site-directed mutagenesis kit (Stratagene, La Jolla, CA) and complementary mutagenic primers as indicated in Table 1. Double-stranded plasmid DNA was heat denatured, and the two mutagenic primers were each simultaneously annealed to their complementary strand. The primers were extended during thermocycling using high-fidelity thermostable *Pfu* DNA polymerase generating copies of the parent plasmid and incorporating the mutation of interest. After an initial denaturation for 3 min at 94 °C, 12 cycles of denaturation for 45 s at 94 °C, annealing for 1 min at 50−65 °C, and extension for 14 min at 72 °C were performed. The annealing temperature was adjusted according to the T_M of the primer pair used. The methylated wild-type DNA was selectively digested with *Dpn*I endonuclease, and a portion of the reaction mixture was used to transform XL1-Blue *E. coli* competent cells. Mutations were confirmed by sequence analysis, and restriction fragments containing PCR-generated mutations were cassetted into the parent expression plasmid to avoid the potential for deleterious mutations elsewhere in the cDNA or plasmid. The double mutants 2C19:V288E, I289N,[3] 2C19:N286S, I289N, and 2C19:N286S, V288E were made by inserting synthesized double-stranded DNA (see Table 1) with *Eco*RI and *Pst*I single-strand overhangs into pCW2C19. Competent *E. coli* XL-1 Blue cells were transformed with ligation products. Selected positive clones were verified by restriction mapping and by sequencing across the inserted fragment.

Table 1: Sequence of Oligonucleotides (A) and Synthetic dsDNA (B) Employed in the Generation of P450 2C9/2C19 Chimeras and Mutants[a]

A:	*Primers employed for site-directed mutagenesis:*
2C9:281*EcoR*I	5′-CAACCATCTGAATT*C*ACTATTGAAAGCTTG-3′ 3′-GTTGGTAGACTTAA*G*TGATAACTTTCGAAC-5′
2C19:E241K	5′-CCTTGCTTTTATG*AAA*AGTGATATTTTGG-3′ 3′-GGAACGAAAATAC*TTT*TCACTATAAAACC-5′
2C19:N286S	5′-GAATTCACTATTGAAA*GC*TTGGTAATCACTGC-3′ 3′-CTTAAGTGATAACTT*TCG*AACCATTAGTGACG-5′
2C19:V288E	5′-CTATTGAAAACTTGG*AA*ATCACTGCAGCTGAC-3′ 3′-GATAACTTTTGAACC*TT*TAGTGACGTCGACTG-5′
2C19:I289N	5′-CTATTGAAAACTTGGTA*AAC*ACTGCAGCTGACTTAC-3′ 3′-GATAACTTTTGAACCAT*TTG*TGACGTCGACTGAATG-5′
B:	*Synthetic dsDNA with EcoRI and PstI overhangs:*
2C19:V288E, I289N	5′-AATTCACTATTGAAAACTTGG*AAAAC*ACTGCA-3′ 3′-GTGATAACTTTTGAACC*TTTTG*TG-5′
2C19:N286S, I289N	5′-AATTCACTATTGAAA*GC*TTGGTTA*AC*ACTGCA-3′ 3′-GTGATAACTTT*TCG*AACCAAT*TG*TG-5′
2C19:N286S, V288E	5′-AATTCACTATTGAAA*GC*TTGG*AA*ATCACTGCA-3′ 3′-GTGATAACTTT*TCG*AACC*TT*TAGTG-5′

[a] Nucleotides highlighted by italic characters indicate mismatched bases relative to the cDNA. Codons for the changed amino acids are underlined.

Heterologous Expression in E. coli and Partial Purification of Recombinant P450s. Protein expression in the transformed *E. coli* XL-1 Blue cells was induced by the addition of IPTG (1 mM final concentration), and the cultures were grown at 30 °C in Terrific Broth under conditions that had previously been optimized for the expression of P450s 2C9 and 2C19 (*2*). Membranes were prepared from the harvested cells, and the recombinant P450s were solubilized and partially purified by hydroxylapatite (HA) chromatography as described for P450s 2C9 and 2C19 (*2*) with the following modification: 0.3% (w/v) CHAPS was added to the elution buffer containing 0.5 M potassium phosphate, pH 7.4, 0.1 mM EDTA, and 20% (v/v) glycerol. Recombinant P450s were stored in this buffer at −80 °C until use. The addition of 0.3% CHAPS was found to increase the yield from HA and to prevent aggregation of P450s in the spectral titration experiments. The presence of CHAPS at the concentrations that occurred following dilution in the assay

[3] Mutants are identified by the single-letter code of the amino acid replaced, the position in the protein sequence, and the single-letter code of the new residue.

mixture did not interfere with the reconstitution of warfarin metabolism as judged by comparisons of 2C9 and 2C19 prepared with and without CHAPS.

Determination of Sulfaphenazole Binding Constants by Visible Difference Spectroscopy. SFZ binding spectra were recorded at ambient temperature with a Varian Cary 1E UV/vis spectrophotometer (Varian, Mulgrave, Victoria, Australia) using a scan rate of 60 nm/min and a spectral bandwidth of 4.0 nm (data interval 0.5 nm). Partially purified P450 preparations were diluted to a final concentration of 0.5−1.0 μM in 0.5 M potassium phosphate buffer, pH 7.4, 20% glycerol, and 0.3% CHAPS. The diluted samples were divided equally between two 1.0 mL quartz cuvettes (1 cm path length), and a baseline was recorded (460−350 nm). Aliquots of SFZ stock solutions in DMSO or EtOH were added to the sample cuvette. The corresponding amount of solvent was added to the reference cuvette (final concentrations were <3% and 1% v/v, respectively, for DMSO and EtOH). Binding was monitored as the absorbance difference, ΔA, between the peak and trough of the difference spectrum (*18*). The apparent equilibrium binding constant, K_s, and the extrapolated maximum spectral change, ΔA_{max}, were estimated from nonlinear least-squares regression fitting (Slide Write Plus, Advanced Graphics Software, Carlsbad, CA) of the following equation:

$$\Delta A = \frac{\Delta A_{max}}{2P}\left[P + S + K_s - \sqrt{(P + S + K_s)^2 - 4PS}\right]$$

where S is the concentration of sulfaphenazole and P is the concentration of the P450.

Warfarin Hydroxylase Assay. (*S*)- and (*R*)-warfarin metabolism was assayed using modified published procedures (*6*, *19*). Complete incubation mixtures (total volume 250 μL) contained 0.1 μM P450, 3 units/mL P450 reductase (1 unit = 1 μmol cytochrome *c* reduced per min at 30 °C), 30 μg/mL L-α-dilauroyl-phosphatidylcholine, 1 mM NADPH, 5 mM isocitrate, 0.5 units/mL isocitrate dehydrogenase, 5 mM $MgCl_2$, 1−500 μM (*S*)- or (*R*)-warfarin (sodium salt), and 500 units/mL catalase (from bovine liver, Sigma) in 50 mM potassium phosphate buffer, pH 7.4. P450 reductase was purified from rabbit liver microsomes or from *E. coli* membranes containing expressed recombinant human P450 reductase as previously described (*20*, *21*). Control incubations omitted either cofactor, P450, reductase, or substrate, respectively. After HPLC analysis, none of the control incubations revealed background peaks that would interfere with the quantification of metabolites. Catalase was added in order to suppress oxidations by reactive oxygen species generated in the reconstitution system. Reactions were carried out at 37 °C and were initiated by the addition of NADPH. After 15−60 min (formation of metabolites was shown to be linear over this period), reactions were terminated by three extractions with 500 μL of ethyl acetate. The extraction efficiency amounted to 80% or greater for all metabolites. The extracts were dried in a speed vac, and the residue was dissolved in 100 μL of 50 mM NH_4OAC, pH 4.0, and 35% acetonitrile. Aliquots (50 μL) were subjected to HPLC analysis on a Nova-Pak C18 column (150 mm length, 3.9 mm i.d., particle size 5 μm, Waters, Milford, MA) using a Beckman 507e autosampler (Beckman, Fullerton, CA). Separation of warfarin and of 4′-, 6-, 7-, and 8-hydroxywarfarin was achieved under isocratic conditions using 50 mM ammonium acetate buffer, pH 4.0, and 35% (v/v) acetonitrile as the mobile phase at a flow rate of 1.0 mL/min delivered with a Beckman 127 HPLC pump. The retention times were 4.7, 5.8, 7.2, and 7.6 min for 4′-, 6-, 7-, and 8-hydroxywarfarin, respectively, and 16.5 min for warfarin. Metabolites were detected by UV absorption at 313 nm using a Beckman 166 UV detector and were identified by coelution with the synthetic reference compounds. Absorbance data were collected and analyzed using a HP 3395 integrator (Hewlett-Packard, Palo Alto, CA). Standard curves were constructed in the concentration range of interest. Linearity ($r > 0.998$) was obtained in each case. Metabolite concentrations were determined by comparing the heights of metabolite peaks with the data comprising the calibration curves.

Inhibition Experiments. IC_{50}s for the inhibition by SFZ of (*S*)-warfarin metabolism by P450s 2C9, 2C19, and 2C19: E241K, N286S, I289N were determined at 6, 120, and 6 μM of (*S*)-warfarin, respectively. SFZ was added to the incubation mixtures in DMSO (final concentration 1% v/v). The residual (*S*)-warfarin 7-hydroxylase activity relative to a control incubation containing 1% DMSO was plotted versus the concentration of SFZ. IC_{50}s were estimated by curve fit analysis.

Additional Analytical Procedures. Protein concentrations were determined using a BCA reagent kit (Pierce Biochemicals, Rockford, IL). P450 concentrations were determined by the method of Omura and Sato (*22*).

Molecular Modeling. A heavy atom model of P450 2C9 was generated by the program MODELLER (*23*) using the structure of P450 BM3 (PDB: 1FAG) complexed with substrate (*24*) as a template. Hydrogens were added to the structure in INSIGHT II (MSI, San Diego, CA) and optimized by minimization using DISCOVER with all heavy atoms fixed. SFZ was built from fragments in INSIGHT II, and the structure was energy-minimized using the MSI constant valence force field. The partial charges were calculated using MOPAC in INSIGHT II. Comparative studies of spectral interaction and inhibitory effects of 12 SFZ derivatives have shown that the aniline function of SFZ is responsible for the formation of the Fe−N bond and for the inhibitory effects of SFZ (*16*). Therefore, SFZ was manually docked in the active site of the 2C9 model with the aniline nitrogen fixed at ∼2 Å above the iron, a typical bond length for porphyrin Fe (III)-N (alkylamine) complexes (*25*) and the phenyl ring positioned above the aniline ring as described by Poli-Scaife et al. (*26*). The orientation of the SFZ molecule was manually adjusted to preclude unfavorable van der Waals interactions with the protein in INSIGHT II.

RESULTS

The binding of sulfaphenazole (SFZ) to P450 2C9 could be monitored directly in membranes prepared from *E. coli* expressing the enzyme by the appearance of a type II difference spectrum with a peak at 424 nm and a trough at 390 nm (Figure 1A). Analysis of the spectral changes elicited by SFZ indicated an apparent K_s of <0.5 μM and a ΔA_{max}/(μM P450) of 0.035. The spectral changes increased linearly at SFZ concentrations that were less than the

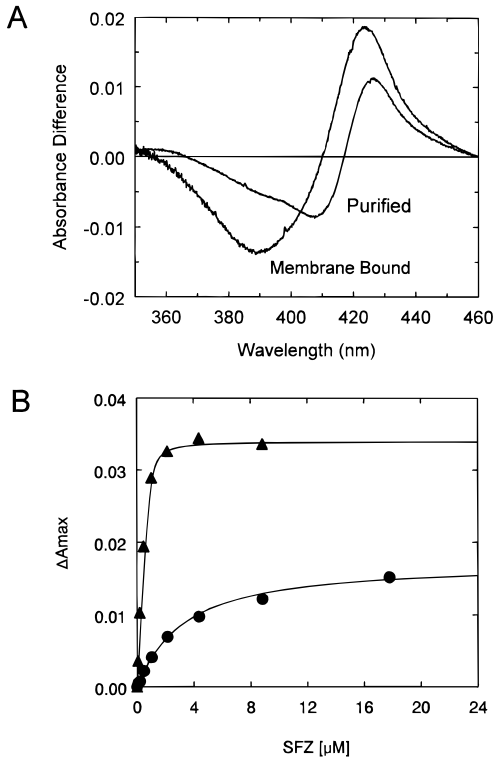

FIGURE 1: Sulfaphenazole-induced spectral changes. (A) The maximal difference spectra obtained by addition of SFZ are shown for a preparation of *E. coli* membranes containing expressed recombinant P450 2C9, 1 μM, and for a preparation of P450 2C9, 1 μM, solubilized using detergents and partially purified by adsorption to and elution from hydroxylapatite. The buffer contained 0.5 M KPi, pH 7.4, 20% glycerol, 0.1 mM EDTA, and in the case of the solubilized enzyme, 0.3% CHAPS. (B) Titration curves depicting the change in absorbance versus the concentration of SFZ for the same preparations of membranes (triangles) and purified protein (circles) used in panel A. The curves were calculated as described in the text.

concentration of the enzyme and did not change significantly at SFZ concentrations that exceeded the concentration of the enzyme (Figure 1B). These results are consistent with relatively tight binding and a 1:1 stoichiometry. The wavelengths of the maximum and minimum difference, the ΔA_{max}/(μM P450), and the value of K_s are highly similar to that reported for P450 2C9 expressed heterologously in yeast microsomes (*16*). In contrast, membranes containing expressed recombinant P450 2C19 gave only a very weak type II binding spectrum with an apparent $K_S \gg 100$ μM (data not shown).

To define which of the 43 of 490 amino acid differences between P450 2C9 and 2C19 contribute to this difference in affinity for SFZ, a series of chimeras were generated to localize specific portions of the P450 2C9 polypeptide chain that could confer high-affinity binding, $K_s < 15$ μM, to the chimera. Several chimeras were expressed at relatively low levels, and the turbidity of the membrane samples prevented spectral analysis of the binding. For this reason, the P450s were solubilized from the membrane with the nonionic detergent Nonidet P40 and partially purified by adsorption to and elution from hydroxylapatite as described (*2*). For many P450s, the enzyme can be washed with detergent-free buffer while adsorbed to the hydroxylapatite and then eluted in detergent-free buffer in order to extensively lower the concentration of the detergent to levels that do not interfere

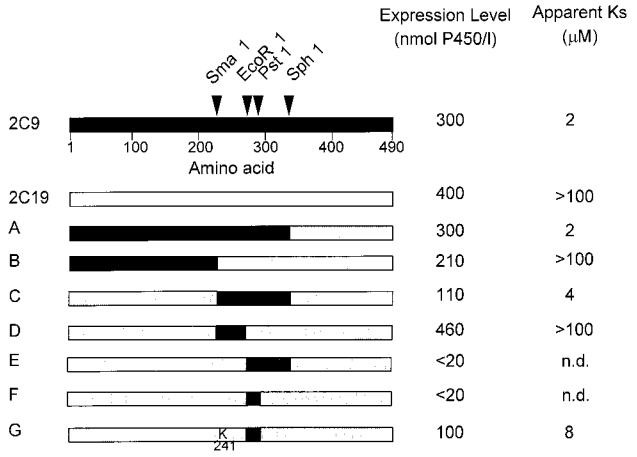

FIGURE 2: Sulfaphenazole binding constants of partially purified P450s 2C9, 2C19 and chimeric proteins expressed in *Escherichia coli*. The left column identifies each hybrid protein according to the nomenclature used in the text. Chimeras are represented by combinations of solid and stippled segments that correspond to the wild-type proteins P450 2C9 or 2C19, respectively. Splice sites used for the construction of chimeric proteins are indicated at the top by arrows: *Sma*I (codon 227); *Eco*RI (codon 281), this restriction site was introduced into 2C9 by a silent mutation (Table 1); *Pst*I (codon 291); and *Sph*I (codon 338). P450 expression levels were determined from whole cell CO difference spectra. The right column shows the apparent spectral dissociation constant (K_S, in μM) for SFZ obtained from spectral titrations of the partially purified recombinant proteins. In some cases, K_S values could not be determined because of low expression levels (n.d.).

with the subsequent reconstitution of the enzyme with reductase. However, the elution of several of the chimeras could not be achieved in sufficient yields using this method, and the inclusion of 0.3% CHAPS in the elution buffer was found to greatly improve the yield. The concentration of CHAPS could then be reduced by dialysis and dilution.

This treatment was observed to have a significant effect on SFZ binding to P450 2C9. As shown in Figure 1A, the resulting difference spectrum of the partially purified preparation differed from that obtained for the membrane sample by exhibiting a slightly higher wavelength of maximum positive change, 426 nm, and a broad bifurcated trough exhibiting a maximum negative change in absorbance at 410 nm. The titration of the partially purified enzyme exhibited a lower ΔA_{max}/(μM P450) of about 0.02 and a higher apparent value of K_s, 2 μM. Reduction of the concentration of CHAPS did not significantly alter these results. Despite this change in the spectrum, the partial purification of the chimeric proteins indicated that several depicted in Figure 2 exhibited apparent K_s values for SFZ binding of <10 μM.

The 2C9/2C19 hybrid protein containing the first 338 N-terminal amino acids of 2C9 (chimera A) showed high-affinity SFZ binding, while the hybrid containing only the first 227 amino acids of 2C9 (chimera B) showed a very low affinity for SFZ. Replacement of amino acids 228−338 (*Sma-Sph*) in 2C19 by the respective 2C9 segment also resulted in a high affinity for SFZ (chimera C). However, substitution of amino acids 228−282 did not yield significant SFZ binding (chimera D). Replacement of amino acids 283−338 or 283−291 with those found in P450 2C9 resulted in extremely low holoenzyme expression levels precluding determination of SFZ binding constants for these hybrids (chimeras E and F).

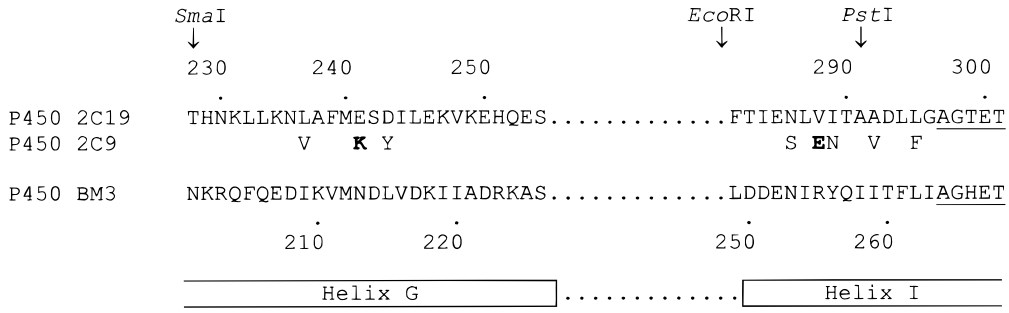

FIGURE 3: Alignment of relevant portions of the amino acid sequences of P450 2C19 and P450 2C9 with the sequence of P450 BM3. The identity of each amino acid sequence is indicated on the left, and the position is shown immediately above and below the sequences for 2C19 and P450 BM3, respectively. For the 2C9 sequence, only the amino acids differing from 2C19 are shown. Restriction sites used for the construction of chimeric proteins are indicated at the top. An additional substitution, E241K, allowing for a favorable charge pair/hydrogen bond interaction between K241 and E288 and N289 (see Figure 4) was essential to achieve expression of the minimal chimera, G. Amino acids that were found to be important for protein stability are highlighted by bold typeface. The secondary structure determined for P450 BM3 is shown below the alignment. The highly conserved A(A/G)XXT motif is underlined.

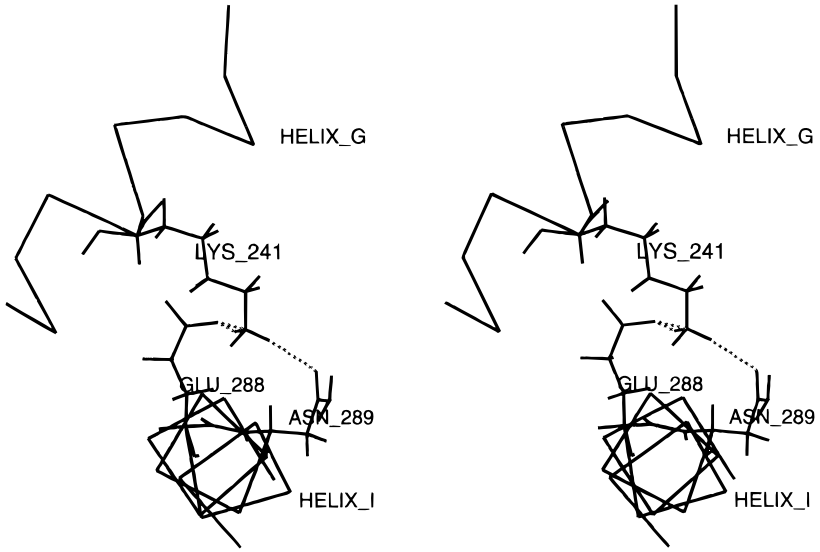

FIGURE 4: Stereo image of a portion of the homology model of P450 2C9 built on the structure of P450 BM3 showing the putative salt bridge and hydrogen bond network between residues K241 in helix G and E288, N289 in helix I. The homology model of P450 2C9 was built as described in Materials and Methods. After adding hydrogens to the model, the side chains for amino acids K241, E288, and N289 were energy-minimized with the remainder of the molecule constrained. The energy-minimized structure indicates that the three residues could form a hydrogen bonding network (dotted lines) in this model based on P450 BM3 as a template.

Relative to chimera C, the loss of stable expression by chimeras E and F suggested the possibility of an unfavorable interaction between the three amino acid residues derived from P450 2C9 within the 283−291 segment and residues 228−282 of P450 2C19. Alignment of the amino acid sequences of P450s 2C19 and 2C9 with that of P450 BM3 (Figure 3) shows that the three differences within the 283−291 segment derived from P450 2C9 by exchange of the *Eco*RI-*Pst*I fragment are likely to reside within helix I. A homology model of P450 2C9 (Figure 4) built on the structure of P450 BM3 suggested a possible ion pair and hydrogen bond interaction between residues E288 and N289 in helix I of P450 2C9 and residue K241 in helix G (Figure 3). Harlow et al. (*27*) recently reported that charge pairing between the corresponding residues of P450 2B11, D290 and K242, is important for protein stability reflecting a need to accommodate the buried, charged residue on the I-helix. Thus, it seemed possible that the negative charges of E241 in 2C19 and E288 derived from 2C9 would interfere in chimeras E and F leading to their poor expression. Indeed, after introduction of the additional substitution E241K, the resulting chimera G was successfully expressed and displayed a K_S of 8 μM (Figure 2). In addition, examination of other mutants, Figure 5, indicated that elimination of the V288E substitution resulted in high expression that did not require the K241E substitution.

Mutants. Chimera G differs from P450 2C19 by only four amino acids. To explore the minimal combination of altered residues that would confer high-affinity SFZ binding, the remaining differing amino acids were systematically replaced with those found in 2C19 (Figure 5). Both the KSN mutant (2C19:E241K, N286S, and I289N) and the SN mutant (2C19: N286S and I289N) exhibited the lowest K_S of ~4 μM. A similar value was determined from the titration of the mutant protein in membranes as shown for the KSN mutant in Figure 6. The maximum and minimum wavelengths for the type II difference spectra of both the purified and membrane-bound enzymes are similar to those of membrane-bound P450 2C9 with a maximum at 424 nm and minimum at 390 nm. This was generally true of all of the chimeric proteins examined with the exception of chimera A, which displayed the altered spectrum following partial purification that was seen for P450 2C9. The other amino acid combinations did not show high-affinity binding, giving K_S values of 50 μM

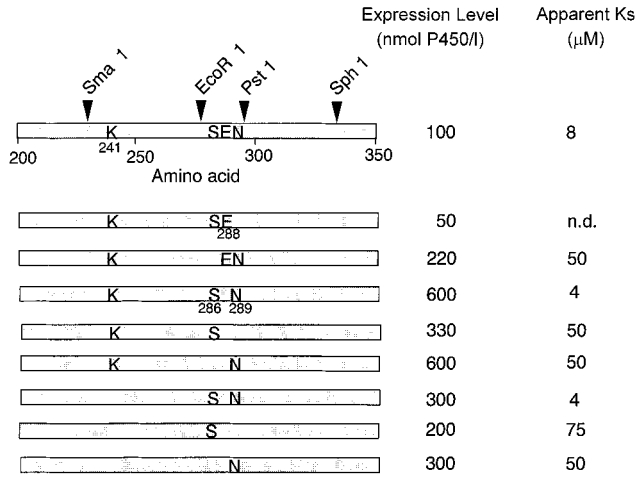

FIGURE 5: Sulfaphenazole binding constants of partially purified P450 2C19 mutants. P450 expression levels were determined from whole cell CO difference spectra. The right column shows the apparent spectral dissociation constants (K_S, in μM) for SFZ obtained from spectral titrations of the partially purified recombinant proteins. In some cases, K_S values could not be determined because of low expression levels (n.d.).

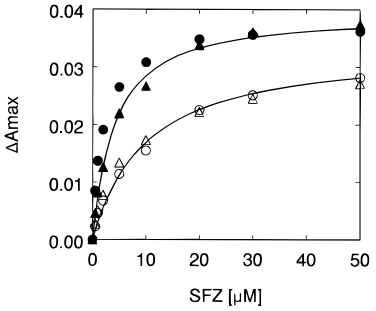

FIGURE 6: Concentration and salt dependence of spectral changes resulting from sulfaphenazole binding to the KSN mutant, P450 2C19:E241K, N286S, I289N. The assays utilized either 1 μM of partially purified P450 2C19:E241K, N286S, I289N protein (circles) or a membrane preparation (triangles) with an equivalent amount of this enzyme in either 0.5 M (closed symbols) or 0.05 M (open symbols) potassium phosphate buffer, pH 7.4, 20% (v/v) glycerol, 0.1 mM EDTA. The purified protein solution also contained 0.3% CHAPS. An equal volume of enzyme solution was placed in both the sample and the reference cuvettes. Aliquots of SFZ stock solutions in EtOH were added to the sample cuvette, and the corresponding amount of EtOH was added to the reference cuvette (final EtOH concentration <1% v/v). The titration curves depict the change in absorbance versus the concentration of sulfaphenazole, SFZ. The continuous curves were fit to the data for the membrane preparation.

or greater (Figure 5). SFZ binding to the KSN and SN mutants was salt-dependent. Lowering of the phosphate concentration from 500 to 50 mM increased the apparent K_S to 9 μM for both membrane and partially purified preparations as shown for the KSN mutant in Figure 6.

Warfarin Metabolism. The regiospecific and stereospecific hydroxylation of (*R*) and (*S*)-warfarin was characterized for both the KSN and SN mutants and compared to that of P450s 2C9 and 2C19. In general, both the KSN and SN mutants of 2C19 exhibited the capacity of P450 2C19 to metabolize both (*R*)- and (*S*)-warfarin with a broad regiospecificity (Figure 7). However, the turnover number exhibited by the KSN mutant was much higher than that of the SN mutant indicating that the E241K mutation contributes to the catalytic activity of the enzyme. More detailed characterization of the kinetic properties of the KSN mutant revealed a dramatic reduction in the apparent K_m for both (*R*) and (*S*)-warfarin to values that approached those exhibited by P450 2C9 for (*S*)-warfarin (Tables 2 and 3). Thus, the low K_m and high V_{max} result in greatly increased catalytic efficiency (V_{max}/K_m) relative to P450 2C19.

All of the chimeric proteins were catalytically active for warfarin metabolism. Chimera A resembled 2C9 in that it

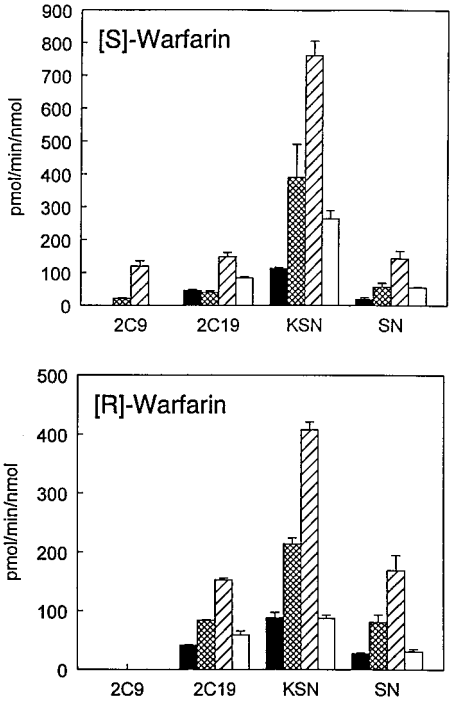

FIGURE 7: Warfarin metabolism catalyzed by P450s 2C9, 2C19, 2C19: E241K, N286S, I289N and 2C19: N286S, I289N. The regiospecificity and stereospecificity for warfarin metabolism by the 2C19 triple mutant (KSN) and the 2C19 double mutant (SN) were compared to the activities obtained with P450s 2C9 and 2C19. A substrate concentration of 100 μM was used, and metabolites were quantified as described in Materials and Methods. The identity of the (*S*)- or (*R*)-warfarin metabolites corresponds to the following: 4′-OH (filled bars), 6-OH (crosshatch bars), 7-OH (diagonal bars), and 8-OH (open bars).

Table 2: Kinetic Characteristics for (*S*)-Warfarin Metabolism by P450s 2C9, 2C19 and 2C19:E241K, N286S, I289N[a]

activity	2C9	2C19	2C19:E241K, N286S, I289N
(*S*)-warfarin-4′-OH			
V_{max} (1000 min^{-1})	nd[b]	85 ± 33	122 ± 2
K_M (μM)		78 ± 33	9 ± 3
(*S*)-warfarin-6-OH			
V_{max} (1000 min^{-1})	24 ± 5	74 ± 21	416 ± 107
K_M (μM)	4 ± 2	82 ± 33	7 ± 2
(*S*)-warfarin-7-OH	105 ± 14	311 ± 57	807 ± 46
V_{max} (1000 min^{-1})	5 ± 1	94 ± 25	
K_M (μM)			
(*S*)-warfarin-8-OH			8 ± 2
V_{max} (1000 min^{-1})	nd	152 ± 18	288 ± 27
K_M (μM)		91 ± 18	9 ± 2

[a] V_{max} and K_M values were estimated by nonlinear regression analysis of the velocity versus substrate concentration plots (concentration range 1−500 μM) and are indicated in the table ± standard errors. Incubation times were limited to 60 min for 2C9 and 2C19 and to 15 min for the 2C19 triple mutant. The times were adjusted in order to avoid excessive substrate depletion. [b] nd, not detected (rates <5 pmol min^{-1} (nmol of P450)$^{-1}$ at 100 μM substrate concentration).

Table 3: Kinetic Characteristics for (*R*)-Warfarin Metabolism by P450s 2C9, 2C19 and 2C19:E241K, N286S, I289N

activity	2C9	2C19	2C19:E241K, N286S, I289N
(*R*)-warfarin-4′-OH			
V_{max} (1000 min^{-1})	nd[a]	97 ± 24	120 ± 13
K_M (μM)		59 ± 25	24 ± 7
(*R*)-warfarin-6-OH			
V_{max} (1000 min^{-1})	nd	168 ± 34	375 ± 69
K_M (μM)		51 ± 18	31 ± 4
(*R*)-warfarin-7-OH			
V_{max} (1000 min^{-1})	nd	329 ± 62	733 ± 137
K_M (μM)		55 ± 18	31 ± 5
(*R*)-warfarin-8-OH			
V_{max} (1000 min^{-1})	nd	300 ± 49	176 ± 55
K_M (μM)		53 ± 15	16 ± 4

[a] nd, not detected (rates <5 pmol min^{-1} (nmol of P450)$^{-1}$ at 100 μM substrate concentration).

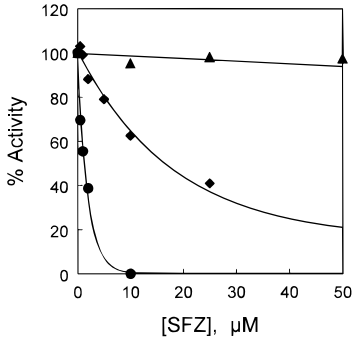

FIGURE 8: Inhibition by sulfaphenazole of (*S*)-warfarin metabolism catalyzed by P450s 2C9, 2C19, or the triple mutant 2C19:E241K, N286S, I289N. Sulafaphenazole (SFZ) inhibition of (*S*)-warfarin metabolism by P450s 2C9 (circles), 2C19 (triangles), and 2C19: E241K, N286S, I289N (diamonds) was determined using substrate concentrations that approximated the estimated K_M values determined for each of the enzymes. SFZ was added in DMSO (final concentrated 1% v/v). Activities are expressed as a percentage relative to control incubations containing 1% DMSO.

only oxidized the (*S*)-enantiomer of warfarin in the 6- and 7-positions. In contrast, chimera C oxidized both (*S*)- and (*R*)-warfarin in the 4′, 6, 7, and 8 positions generating a metabolite profile similar to 2C19. These results indicate that residues upstream of amino acid 228 are important for the regiospecificity and stereospecificity of warfarin metabolism.

Inhibition Studies. To provide complementary information to the spectral studies, the effect of SFZ on (*S*)-warfarin 7-hydroxylase activity was determined for the KSN mutant (2C19:E241K, N286S, I289N) and compared to the data obtained with the wild-type proteins 2C9 and 2C19 (Figure 8). The substrate concentration used for each enzyme was chosen on the basis of estimates of the K_m of the enzyme. The IC_{50} value for the inhibition by SFZ of 2C9-dependent (*S*)-warfarin 7-hydroxylase activity, 1.3 μM, was very similar to the spectral binding constant exhibited by the purified protein for SFZ, 2.3 μM, indicating that the inhibitory effects of SFZ on P450 2C9 metabolism should result from binding as an iron ligand. In agreement with the low affinity observed in the spectral titrations, 2C19-dependent (*S*)-warfarin metabolism was not significantly inhibited by SFZ at concentrations up to 100 μM. The KSN mutant that showed high-affinity SFZ binding in the spectral titrations and high catalytic efficiency also had a dramatically lowered IC_{50} for warfarin metabolism ($IC_{50} \sim 15$ μM). This value is consistent with the value of 9 μM determined from the spectral studies under similar conditions of low ionic strength.

DISCUSSION

Chimeric proteins between P450s 2C9 and 2C19 were screened in order to identify which of the 43 differences of amino acid sequence underlie the large differences in binding affinity for the selective inhibitor of 2C9, sulfaphenazole (SFZ). This strategy demonstrated that two substitutions, N286S and I289N in P450 2C19 were sufficient to confer high-affinity SFZ binding (<4 μM). When combined with a third substitution, E241K, the resulting triple mutant exhibited a high catalytic efficiency for hydroxylation of (*R*)- and (*S*)-warfarin exhibiting a low K_m similar to that of P450 2C9. The apparent binding constant of the KSN and SN mutants is roughly 10-fold higher than that of P450 2C9 as determined in this study, <0.5 μM, and as reported by Mancy et al. (*16*), 0.3 μM.

Previous studies of this nature (*28*) have generally identified specific amino acid differences between closely related P450s that fall within putative substrate recognition sites (SRS) (*29*) that roughly correspond to the positions of substrate contact residues observed in P450 cam when the sequences of mammalian P450 family 2 enzymes are aligned with that of P450 cam. The critical differences N286S and I289N identified in this study reside in SRS 4 as originally defined by Gotoh (*29*). However, on the basis of homology modeling, it is unlikely that these residues directly contact the substrate.

Residues 286 and 289 occur in a region corresponding to helix I of structurally characterized P450s. There is a general consensus in the alignment of mammalian sequences with that of helix I due to the occurrence of a highly conserved sequence motif, (A/G)GXXT (Figure 3) that occurs in close proximity to the heme iron and that is also present in SRS 4. Thus, the locations of the amino acid differences relative to the active site can be predicted with significant confidence. When modeled using this alignment and the structure of P450 BM3 as a template, the N286S difference is roughly 18 Å from the heme iron. Examination of each of the known structures of P450s indicates that the loop between helix B′ and helix C generally passes between this residue and the active site forming a barrier between the substrate and this residue. This can be seen for the homology model based on a P450 BM3 template (Figure 9). Thus, it is unlikely that the N286S substitution directly alters the size and shape of the active site cavity of the enzyme by changes in the volume of the side chain. This is consistent with the observed retention by the 2C19 KSN mutant of the regiospecificity exhibited by wild-type P450 2C19 for the hydroxylation of both (*S*)- and (*R*)-warfarin.

In addition, the homology model suggests that the I289N difference lies at the interface of helix I with helix G (Figure 9). Helix G along with helix F forms the upper boundary of the substrate binding cavity. In general, helices F and G exhibit high temperature factors in experimentally determined P450 structures (*30*), and for P450 BM3, each of the two molecules in the unit cell exhibit relatively large differences in the positions of the F and G helices (*31*) that are also altered upon substrate binding (*24*). Molecular dynamics

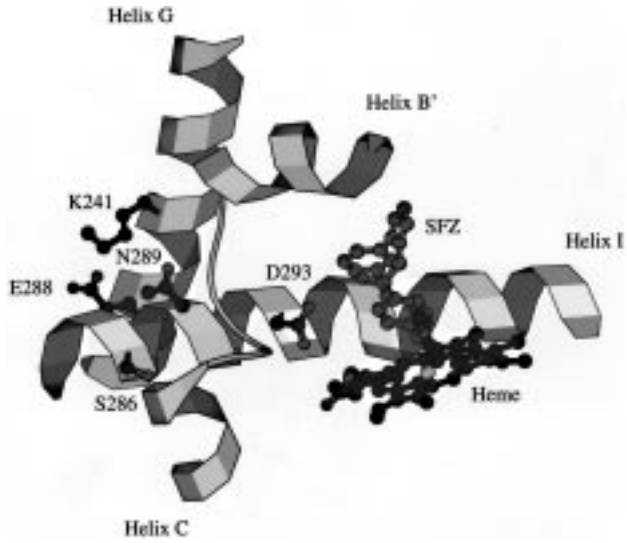

FIGURE 9: Sulfaphenazole docked into the active site model of P450 2C9. The aniline nitrogen of SFZ was fixed at a distance of 2 Å from the heme iron, a typical bond length for P450−Fe−N bonds (*25*). The position of the phenyl ring is similar to that proposed by Poli-Scaife et al. (*26*) based on distances determined by NMR for the binding of other substrates to P450 2C9. The binding cavity of the molecule is sufficiently large to accommodate SFZ in the orientation shown without any significant van der Waals overlaps with the protein. The figure clearly demonstrates that residues K241, S286, and N289, which together confer high-affinity SFZ binding to 2C19, are too far away from the heme iron in this homology model to be in direct contact with the bound inhibitor. D293, which is in close proximity to the substrate, is shown. Portions of helices B′, C, G, and I are depicted as ribbons. This figure was rendered using the program MOLSCRIPT (*46*).

studies suggest that this "flap" over the active site may exhibit a considerable range of motion (*32*) which may be necessary for substrate access and product egress. It is conceivable, therefore, that alterations of the interface of helix G with helix I, which serves as a pivot point for these motions, could indirectly influence substrate binding by altering the range or rate of motion of the F and G helices and affect substrate interaction. Although these changes did not affect the regiospecificity of warfarin hydroxylation, they did confer a decrease in the apparent K_M for both (*S*)- and (*R*)-warfarin in addition to enabling the high-affinity binding of SFZ.

The alignment of the mammalian P450 sequences with helix G where residue 241 of P450 2C9 resides is more ambiguous than that of helix I. The alignments used to model P450 2D6 by Modi et al. (*33*) and by De Groot et al. (*34*) differ from the alignment that Szklarz et al. (*35*) used to model P450 2B1. The latter is similar to that used by Chang et al. (*36*) to model P450 2B4. In the latter two alignments, the E241K difference would correspond to N213 of P450 BM3 as shown in Figure 3. Examination of molecule B in the unit cell of crystalline P450 BM3 indicates that N213 can hydrogen bond to R255 in helix I. The latter corresponds by these alignments to the V288E difference between P450s 2C9 and 2C19. Harlow et al. (*27*) proposed that residues K242 and D290 of P450 2B11, which correspond to N213 and R255 of P450 BM3, form a charge pair because changing the charge of either residue led to low levels of protein expression unless the reciprocal change of charge was made in the other residue. Although unpaired charged residues are often seen at this alignment position in helix G, this residue always exhibits a complementary charge when a charged residue occurs at the alignment position corresponding to residue 288 of P450 2C9 in helix I. This probably reflects a need to compensate for the buried location of the charged residue on helix I. A similar situation arose in the initial panel of chimeras investigated in this study where poor expression was evident for chimeras E and F, Figure 2, that paired the corresponding residues E288 of P450 2C9 with E241 of P450 2C19. The mutation, E241K, led to successful expression of chimera G, Figure 2. Chimera G differs from P450 2C19 by only four amino acids, E241K, N286S, V288E, and I289N. Our results support the conclusion of Harlow et al. (*27*) that a residue of opposite charge in helix G with a position corresponding to K241 of P450 2C9 may be required when a charged residue is present on helix I at the position corresponding to E288 of P450 2C9. Elimination of this residue in the SN mutant resulted in high expression without the K241E substitution. However, a charged residue at alignment position 241 does not require an opposite charge on helix I for stable expression as evidenced by the KSN and SN mutants where a neutral, hydrophobic residue is present at residue 288 in helix I.

Harlow et al. (*27*) also noted that changing this pair of residues altered the regiospecificity of steroid hydroxylations catalyzed by P450 2B11 and 2B1. The apparent binding constant for SFZ exhibited by the P450 2C19 N286S, I289N double mutant is similar to that of chimera G which contains the salt bridge. Thus, the presence of a salt bridge between residues 241 and 288 is not necessary to confer relatively tight binding for SFZ to P450 2C19. However, the presence of the E241K mutation greatly increased the turnover number of the enzyme for (*S*)- and (*R*)-warfarin hydroxylation.

Several pharmacophore models for P450 2C9 have recently been described that exhibit features consistent with a contribution both from electrostatic or hydrogen bond interactions and from π-stacking interactions between the substrates defining the pharmacophore and P450 2C9 (*37*−*39*). With the exception of phenytoin, most known substrates of P450 2C9 are acidic with pK_a values between 4.5 and 5.7 (*39*). Consequently, one of the pharmacophore models suggests that the interaction of an anionic site on the substrate with a cationic site of the protein is a key feature of the interaction with P450 2C9 (*39*). This concept reflects a situation, with an inversion of charges, analogous to that proposed for the P450 2D6 active site (*40*−*43*). Site-directed mutagenesis studies indicate that D301 of P450 2D6 is required for catalytic activity suggesting that this residue serves as the negatively charged site in P450 2D6 (*44*).

By alignment, this acidic residue is also conserved in P450 2C9 (D293) where it could potentially form hydrogen bonds with the substrate if both D293 and the substrate were protonated (Figure 9). Substrates and amino acid side chains that are normally anionic at physiological pH can have a significantly higher pK_a in the active site binding pocket. Indeed, it has been reported that the pK_a of a given compound can change by over 3 pK_a units when bound in an enzyme active site (*45*). Accordingly, two of the P450 2C9 pharmacophore models (*37*, *38*) assume that the substrates are protonated when bound and that hydrogen bonding between the substrate and protein determines the orientation of the substrate in the active site. In the absence of experimental data providing direct information on the protonation state

of 2C9 substrates in the active site, it is difficult to rule out one of the two possibilities. However, replacement of the carboxylic acid group in tienilic acid, a substrate of P450 2C9, by either an amide, a methylester, or a CH_2OH group prevented oxidation of these substrates by recombinant 2C9 (*39*), which is consistent with the importance of the charged site on the substrate for binding. The amino acid residues identified in this study that confer SFZ binding to P450 2C19 are all capable of hydrogen bonding. Although the homology model indicates that these residues are not likely to fill a role in directly interacting with the substrate, they could participate in hydrogen bonding networks and salt bridges that could contribute to differences in the hydration of the active site and equilibration of protons with acidic and basic moieties of the protein or substrate. This could contribute to the high turnover number for the KSN mutant.

In summary, a two step approach, involving the generation of P450 2C19/2C9 chimeric proteins followed by site-directed mutagenesis, was used to identify three amino acid residues that conferred high-affinity SFZ binding and higher catalytic efficiency for warfarin hydroxylation to 2C19. The generation of hybrid proteins provided an excellent means of identifying key regions of the protein small enough to be systematically examined by site-directed mutagenesis. In the course of this study, the use of a homology model of P450 2C9 was found to be useful in the design of stable hybrid proteins and in the guidance and interpretation of site-directed mutagenesis studies. The homology model suggests that the altered amino acid residues that conferred high-affinity SFZ binding and a low K_M for warfarin metabolism are not likely to be in direct contact with the substrate. However, these changes could affect the substrate access channel or modify the packing of the active site by increasing active site hydration, thereby facilitating the binding of highly polar or ionized substrates.

REFERENCES

1. Romkes, M., Faletto, M. B., Blaisdell, J. A., Raucy, J. L., and Goldstein, J. A. (1991) *Biochemistry 30*, 3247−3255.
2. Richardson, T. H., Jung, F., Griffin, K. J., Wester, M., Raucy, J. L., Kemper, B., Bornheim, L. M., Hassett, C., Omiecinski, C. J., and Johnson, E. F. (1995) *Arch. Biochem. Biophys. 323*, 87−96.
3. Goldstein, J. A., Ishizaki, T., Chiba, K., de Morais, S. M., Bell, D., Krahn, P. M., and Evans, D. A. (1997) *Pharmacogenetics 7*, 59−64.
4. Jung, F., Richardson, T. H., Raucy, J. L., and Johnson, E. F. (1997) *Drug Metab. Dispos. 25*, 133−139.
5. Bajpai, M., Roskos, L. K., Shen, D. D., and Levy, R. H. (1996) *Drug Metab. Dispos. 24*, 1401−1403.
6. Kaminsky, L. S., De Morais, S. M. F., Faletto, M. B., Dunbar, D. A., and Goldstein, J. A. (1993) *Mol. Pharmacol. 43*, 234−239.
7. Rettie, A. E., Korzekwa, K. R., Kunze, K. L., Lawrence, R. F., Eddy, A. C., Aoyama, T., Gelboin, H. V., Gonzalez, F. J., and Trager, W. F. (1992) *Chem. Res. Toxicol. 5*, 54−59.
8. De Morais, S. M. F., Wilkinson, G. R., Blaisdell, J., Nakamura, K., Meyer, U. A., and Goldstein, J. A. (1994) *J. Biol. Chem. 269*, 15419−15422.
9. Goldstein, J. A., Faletto, M. B., Romkes-Sparks, M., Sullivan, T., Kitareewan, S., Raucy, J. L., Lasker, J. M., and Ghanayem, B. I. (1994) *Biochemistry 33*, 1743−1752.
10. Karam, W. G., Goldstein, J. A., Lasker, J. M., and Ghanayem, B. I. (1996) *Drug Metab. Dispos. 24*, 1081−1087.
11. Ibeanu, G. C., Ghanayem, B. I., Linko, P., Li, L. P., Pedersen, L. G., and Goldstein, J. A. (1996) *J. Biol. Chem. 271*, 12496−12501.
12. Miners, J. O., Smith, K. J., Robson, R. A., McManus, M. E., Veronese, M., and Birkett, D. J. (1988) *Biochem. Pharmacol. 37*, 1137−1144.
13. Veronese, M. E., McManus, M. E., Laupattarakasem, P., Miners, J. O., and Birkett, D. J. (1990) *Drug Metab. Dispos. 18*, 356−361.
14. Baldwin, S. J., Bloomer, J. C., Smith, G. J., Ayrton, A. D., Clarke, S. E., and Chenery, R. J. (1995) *Xenobiotica 25*, 261−270.
15. Veronese, M. E., Mackenzie, P. I., Doecke, C. J., McManus, M. E., Miners, J. O., and Birkett, D. J. (1991) *Biochem. Biophys. Res. Commun. 175*, 1112−1118.
16. Mancy, A., Dijols, S., Poli, S., Guengerich, F. P., and Mansuy, D. (1996) *Biochemistry 35*, 16205−16212.
17. Steward, D. J., Haining, R. L., Henne, K. R., Davis, G., Rushmore, T. H., Trager, W. F., and Rettie, A. E. (1997) *Pharmacogenetics 7*, 361−367.
18. Estabrook, R. W., and Werringloer, J. (1978) *Methods Enzymol. 52*, 212−220.
19. Fasco, M. J., Piper, L. J., and Kaminsky, L. S. (1977) *J. Chromatogr. 131*, 365−373.
20. Yasukochi, Y., and Masters, B. S. S. (1976) *J. Biol. Chem. 251*, 5337−5344.
21. Johnson, E. F., Schwab, G. E., and Muller-Eberhard, U. (1979) *Mol. Pharmacol. 15*, 708−717.
22. Omura, T., and Sato, R. (1964) *J. Biol. Chem. 239*, 2379−2385.
23. Sali, A., and Blundell, T. L. (1993) *J. Mol. Biol. 234*, 779−815.
24. Li, H. Y., and Poulos, T. L. (1997) *Nat. Struct. Biol. 4*, 140−146.
25. Mansuy, D., Battioni, P., Chottard, J. C., Riche, C., and Chiaroni, A. (1983) *J. Am. Chem. Soc. 105*, 455−463.
26. Poli-Scaife, S., Attias, R., Dansette, P. M., and Mansuy, D. (1997) *Biochemistry 36*, 12672−12682.
27. Harlow, G. R., He, Y. A., and Halpert, J. R. (1997) *Biochim. Biophys. Acta 1338*, 259−266.
28. Von Wachenfeldt, C., and Johnson, E. F. (1995) in *Cytochrome P450: Structure, Mechanism, and Biochemistry (Second Edition)* (Ortiz de Montellano, P. R., Ed.) pp 183−244, Plenum Press, New York.
29. Gotoh, O. (1992) *J. Biol. Chem. 267*, 83−90.
30. Hasemann, C. A., Kurumbail, R. G., Boddupalli, S. S., Peterson, J. A., and Deisenhofer, J. (1995) *Structure 3*, 41−62.
31. Ravichandran, K. G., Boddupalli, S. S., Hasemann, C. A., Peterson, J. A., and Deisenhofer, J. (1993) *Science 261*, 731−736.
32. Paulsen, M. D., and Ornstein, R. L. (1995) *Proteins 21*, 237−243.
33. Modi, S., Paine, M. J., Sutcliffe, M. J., Lian, L. Y., Primrose, W. U., Wolf, C. R., and Roberts, G. C. K. (1996) *Biochemistry 35*, 4540−4550.
34. De Groot, M. J., Vermeulen, N. P. E., Kramer, J. D., Van Acker, F. A. A., and Den Kelder, G. M. D. O. (1996) *Chem. Res. Toxicol. 9*, 1079−1091.
35. Szklarz, G. D., He, Y. A., and Halpert, J. R. (1995) *Biochemistry 34*, 14312−14322.
36. Chang, Y. T., Stiffelman, O. B., Vakser, I. A., Loew, G. H., Bridges, A., and Waskell, L. (1997) *Protein Eng. 10*, 119−129.
37. Jones, B. C., Hawksworth, G., Horne, V. A., Newlands, A., Morsman, J., Tute, M. S., and Smith, D. A. (1996) *Drug Metab. Dispos. 24*, 260−266.
38. Jones, J. P., He, M. X., Trager, W. F., and Rettie, A. E. (1996) *Drug Metab. Dispos. 24*, 1−6.
39. Mancy, A., Broto, P., Dijols, S., Dansette, P. M., and Mansuy, D. (1995) *Biochemistry 34*, 10365−10375.

40. Wolff, T., Distlerath, L. M., Worthington, M. T., Groopman, J. D., Hammons, G. J., Kadlubar, F. F., Prough, R. A., Martin, M. V., and Guengerich, F. P. (1985) *Cancer Res. 45*, 2116−2122.
41. Meyer, U. A., Gut, J., Kronbach, T., Skoda, C., Meier, U. T., Catin, T., and Dayer, P. (1986) *Xenobiotica 16*, 449−464.
42. Islam, S. A., Wolf, C. R., Lennard, M. S., and Sternberg, M. J. E. (1991) *Carcinogenesis 12*, 2211−2219.
43. Koymans, L., Vermeulen, N. P. E., van Acker, S. A. B. E., te Koppele, J. M., Heykants, J. J. P., Lavrijsen, K., Meuldermans, W., and den Kelder, G. M. D. (1992) *Chem. Res. Toxicol. 5*, 211−219.
44. Mackman, R., Tschirret-Guth, R. A., Smith, G., Hayhurst, G. P., Ellis, S. W., Lennard, R. S., Tucker, G. T., Wolf, C. R., and Ortiz De Montellano, P. R. (1996) *Arch. Biochem. Biophys. 331*, 134−140.
45. Cleland, W. W., and Kreevoy, M. M. (1994) *Science 264*, 1887−1890.
46. Kraulis, P. J. (1991) *J. Appl. Crystallogr. 24*, 946−950.

BI981704C